Chapter 4

Enhanced Single-Phase Laminar Tube-side Flows and Heat Transfer

SUMMARY: This section presents methods for predicting heat transfer and pressure drop for laminar flows inside circular tubes, rectangular channels, spirally fluted tubes, internally ribbed or finned tubes, and in tubes with twisted tape inserts. First of all, an overview of prediction methods for laminar flow and heat transfer in plain tubes and in rectangular channels with high aspect ratios is presented for the reader's convenience. This is followed with a discussion of special effects on laminar flow heat transfer in microchannels, such as axial conduction, viscous heating, etc. Experimental results and prediction methods for laminar flow enhancements are then presented and discussed.

4.1 Introduction

This chapter covers laminar flow and heat transfer inside plain tubes, rectangular channels, microchannels, enhanced tubes and tubes with inserts. The commonly used prediction methods for heat transfer and pressure drop for plain tubes are first presented, followed by methods for rectangular channels (of particular interest to micro-scale heat transfer applications). Then, special effects on laminar flow heat transfer are addressed (axial conduction, viscous dissipation, etc.) and some guidelines are presented to note when these become important. Next, design methods for internally finned and spirally fluted tubes and tubes with twisted tape inserts are presented. The reader is referred to other sources for more detailed reviews of the literature and experimental results, such as the book of Webb (1994), the reviews by Bergles and Joshi (1983) on enhanced heat transfer, and Morini (2008) on special effects on laminar flows.

Tubular enhancements made by Wolverine Tube Inc. include corrugated tubes and tubes with integral internal fins or ribs. In particular, it must be pointed out that such tubes may provide enhancement relative to a plain tube when the fluid in the tube is being heated. Instead, when the fluid is being cooled, such geometries are not as effective because the more viscous cold fluid near the wall tends to hold up between the fins or corrugations and hence negate their effect on the flow. Furthermore, laminar flow enhancement is quite different than turbulent flow in that the fluid in a laminar flow does not "move" or "mix" unless it is forced to flow to the center of the channel or vice-versa. Hence, small ribs, corrugations and fins on internal tube walls that provide an excellent enhancement in a turbulent tubular flow may have little effect on a laminar flow.

Figure 4.1 shows a diagram of a single-start corrugated tube and Figure 4.2 depicts a photograph of a Wolverine Korodense corrugated tube. A corrugated tube is defined geometrically by the corrugation pitch, p, and the corrugation depth, e. The axial corrugation pitch is related to the internal diameter d_i, helix angle β relative to the axis of the tube and the number of starts n_s by the following geometrical equation:

$$p = \frac{\pi\, d_i}{n_s \tan\beta} \qquad [4.1.1]$$

The external diameter over the corrugations on the outside of the tube is equal to that of the plain ends of the tube. The internal diameter is taken as the external diameter less twice the tube wall thickness. The internal area ratio of a corrugated tube relative to a plain tube of the same diameter d_i is slightly larger than one.

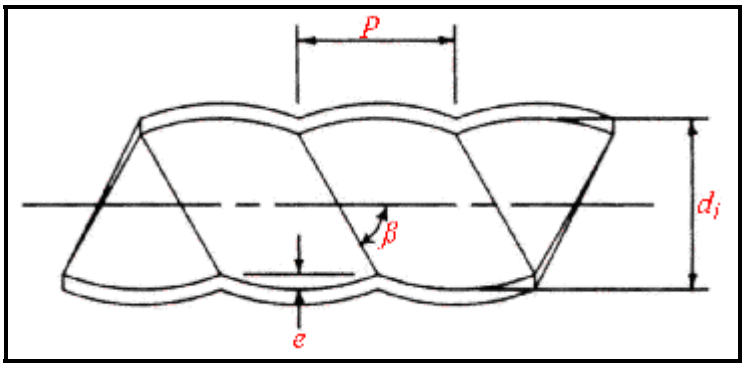

Figure 4.1. Diagram of corrugated tube.

Figure 4.2. Photograph of Wolverine Korodense tube.

Figure 4.3 depicts a schematic diagram for an internally finned or ribbed tube. These two names will be assumed to refer to the same geometry here. Helical internal *fins* or *ribs* (or also referred to as *ridges* in Wolverine Tube literature) are applied to the inside of low finned tubes such as Turbo-Chil and S/T Trufin and to enhanced boiling and condensing tubes, such as the various versions of Turbo-B and Turbo-C. The internal geometry is defined by the fin height, the mean fin thickness, the apex angle of the fin, the helix angle of the fin and the axial pitch of one fin to the next. The helix angle is related to the axial fin pitch by applying the expression above using the number of fins in place of the number of starts. The internal area ratio relative to a plain tube of the same diameter d_i ranges from about 1.3 to 2.0. The internal fins can be of various cross-sectional shapes. Most industrial tubes have fins (or ribs or ridges) with a trapezoidal cross-sectional profile (wider at the base than at the tip of the fin and with rounded corners). Figure 4.4 shows a photograph of a Wolverine Turbo-Chil low finned tube with internal helical fins.

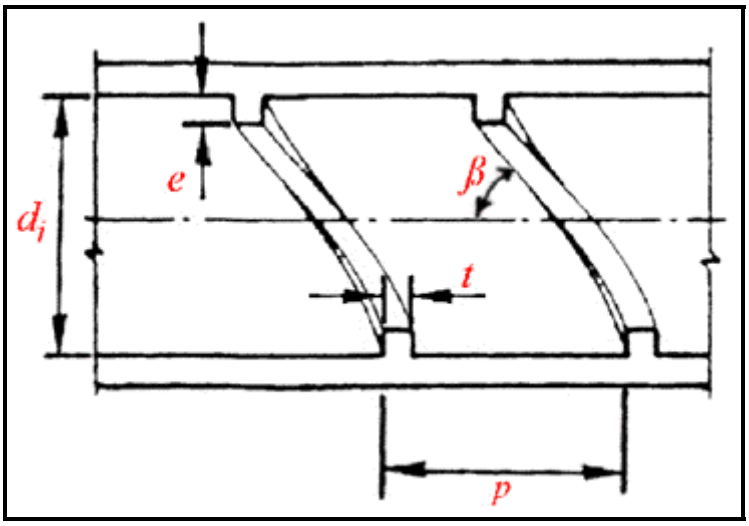

Figure 4.3. Diagram of internally finned or ribbed tube.

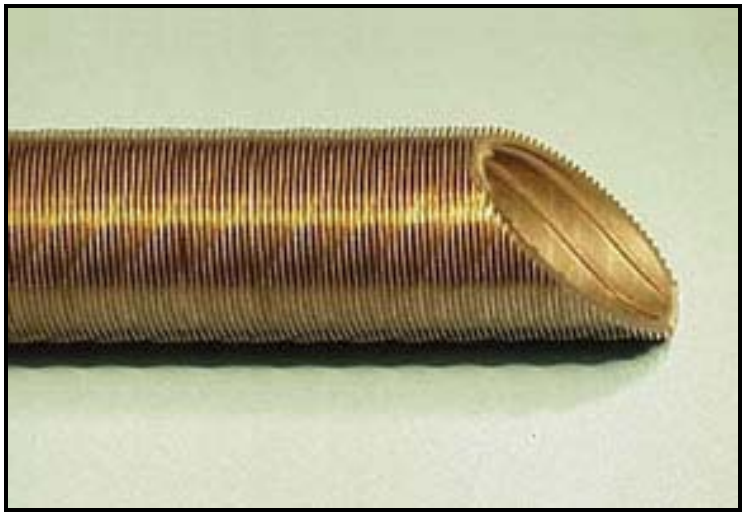

Figure 4.4. Photograph of Wolverine Turbo-Chil tube.

4.2 Transition of Flow and Entrance Shape Effects on Heat Transfer in Plain Tubes

Before discussing heat transfer enhancement of laminar, single-phase flows inside tubes, the effects of the tube inlet configuration on heat transfer and flow regime transition thresholds need to be addressed. For a summary of this topic, the reader is referred to Section 5.2 elsewhere in this book. In generally, laminar flow is normally assumed to occur at Reynolds numbers below 2300 (some also cite 2100); however, this threshold value is a function of the inlet shape among other things and methods for its calculation are given in Section 5.2. This topic has also been addressed by Gnielinski (1995) with propositions for the flow transition regimes and heat transfer methods.

4.3 Laminar Flow and Heat Transfer in Plain Circular Tubes

The most commonly used methods for predicting fully developed laminar flow heat transfer coefficients inside smooth, round tubes can be derived from first principles, which can be found in most textbooks and hence this theory is not reproduced here. For a uniform heat flux wall boundary condition (H) for fully developed laminar flow (both thermally and hydrodynamically), the Nusselt number is given by:

$$Nu_H = \frac{\alpha_{pt}\, d_i}{k} = 4.364 \qquad [4.3.1]$$

The Nusselt number Nu_H is based on the tube diameter d_i and α_{pt} is the convective heat transfer coefficient for a plain tube. As can be seen, the heat transfer coefficient is not a function of the Reynolds number or the Prandtl number. Similarly, for a uniform wall temperature wall boundary condition (T) for fully developed laminar flow, the Nusselt number is given by:

$$Nu_T = \frac{\alpha_{pt}\, d_i}{k} = 3.657 \qquad [4.3.2]$$

Again, the heat transfer coefficient is not a function of the Reynolds or Prandtl numbers. The tubular Reynolds number Re is defined as:

$$Re = \frac{\dot{m}\, d_i}{\mu} \qquad [4.3.3]$$

The mass velocity $\dot{m}$ is in kg/m^{2}s and is obtained by dividing the mass flow rate in kg/s by the cross-sectional area of the tube in m^2. The Prandtl number Pr is obtained from the physical properties of the fluid and is defined as:

$$Pr = \frac{c_p \mu}{k} \qquad [4.3.4]$$

The hydrodynamic entrance length z_{eh} to arrive at fully developed hydrodynamic flow can be estimated by the following expression:

$$\frac{z_{eh}}{d_i} = 0.03\, Re \qquad [4.3.5]$$

The value of 0.03 is used to arrive within 5% of the fully developed laminar friction factor while a value of 0.05 is used to arrive within 1.4% of that value, as is cited in Lienhard and Lienhard (2006). For the thermal developing length when the velocity profile is already fully developed before the heat transfer zone begins, the thermal entrance length z_{et} starting from that location is given by the expression:

$$\frac{z_{et}}{d_i} = 0.034\, Re\, Pr \qquad [4.3.6]$$

Thus, highly viscous flows, such as oils, practically never become fully developed. The value of 0.034 is used to arrive within 5% of the fully developed laminar heat transfer for a constant wall temperature condition while a value of 0.043 is used for a constant heat flux condition. When the velocity and temperature profiles develop simultaneously, the value tends to range between 0.028 and 0.053 depending on the wall condition and the Prandtl number. All of these values are those recommended in Lienhard and Lienhard (2006).

Shah and London (1978) give the analytical solutions to many laminar flow situations for hydrodynamically developing flows, thermally developing flows, simultaneously developing flows, etc. The most comprehensive work in the literature is for circular ducts for thermally developing flow. For practical design, Shah and London (1978) recommend the use of the following expressions for the local value of $Nu_{T,z}$ for a constant wall temperature boundary (T):

$$For\ z^* \le 0.01: \quad Nu_{T,z} = \frac{\alpha_{pt}\, d_i}{k} = 1.077\left(z^*\right)^{-1/3} - 0.1 \qquad [4.3.7a]$$

$$For\ z^* > 0.01: \quad Nu_{T,z} = \frac{\alpha_{pt}\, d_i}{k} = 3.657 + 6.874\left(1000\, z^*\right)^{-0.488} e^{-57.2 z^*} \qquad [4.3.7b]$$

The term z* is a form of the Graetz number based on the length from the entrance of the channel z, given as:

$$z^* = \frac{\pi}{4\,Gz} \qquad [4.3.8]$$

This expression includes the Graetz number, which is defined as:

$$Gz = \frac{Re\, Pr\, d_i}{z} \qquad [4.3.9]$$

For a uniform wall heat flux boundary condition (H), Shah and London (1978) recommend using the following expressions for the local Nusselt number $Nu_{H,z}$:

$$For\ z^* \le 0.00005: \quad Nu_{H,z} = \frac{\alpha_{pt}\, d_i}{k} = 1.302\left(z^*\right)^{-1/3} - 1 \qquad [4.3.10a]$$

$$For\ 0.00005 < z^* \le 0.0015: \quad Nu_{H,z} = \frac{\alpha_{pt}\, d_i}{k} = 1.302\left(z^*\right)^{-1/3} - 0.5 \qquad [4.3.10b]$$

$$For\ z^* > 0.0015: \quad Nu_{H,z} = \frac{\alpha_{pt}\, d_i}{k} = 4.364 + 8.68\left(1000\, z^*\right)^{-0.506} e^{-41 z^*} \qquad [4.3.10c]$$

For simultaneously thermally and hydrodynamically developing flow, Shah and London (1978) recommend the use of the following equation for a constant wall temperature boundary condition (T) for the local Nusselt number $Nu_{T,z}$:

$$\frac{Nu_{T,z}+1.7}{5.357\left\{1+\left[388z^*/\pi\right]^{-8/9}\right\}^{3/8}}=\left[1+\left(\frac{\pi/(284z^*)}{\left\{1+\left(Pr/0.0468\right)^{2/3}\right\}^{1/2}\left\{1+\left(388z^*/\pi\right)^{-8/9}\right\}^{3/4}}\right)^{4/3}\right]^{3/8}$$

[4.3.11]

Similarly for a uniform heat flux boundary condition (H) for simultaneously developing flow, they recommended:

$$\frac{Nu_{H,z}+1}{5.364\left\{1+\left[220z^*/\pi\right]^{-10/9}\right\}^{3/10}}=\left[1+\left(\frac{\pi/(115.2z^*)}{\left\{1+\left(Pr/0.0207\right)^{2/3}\right\}^{1/2}\left\{1+\left(220z^*/\pi\right)^{-10/9}\right\}^{3/5}}\right)^{5/3}\right]^{3/10}$$

[4.3.12]

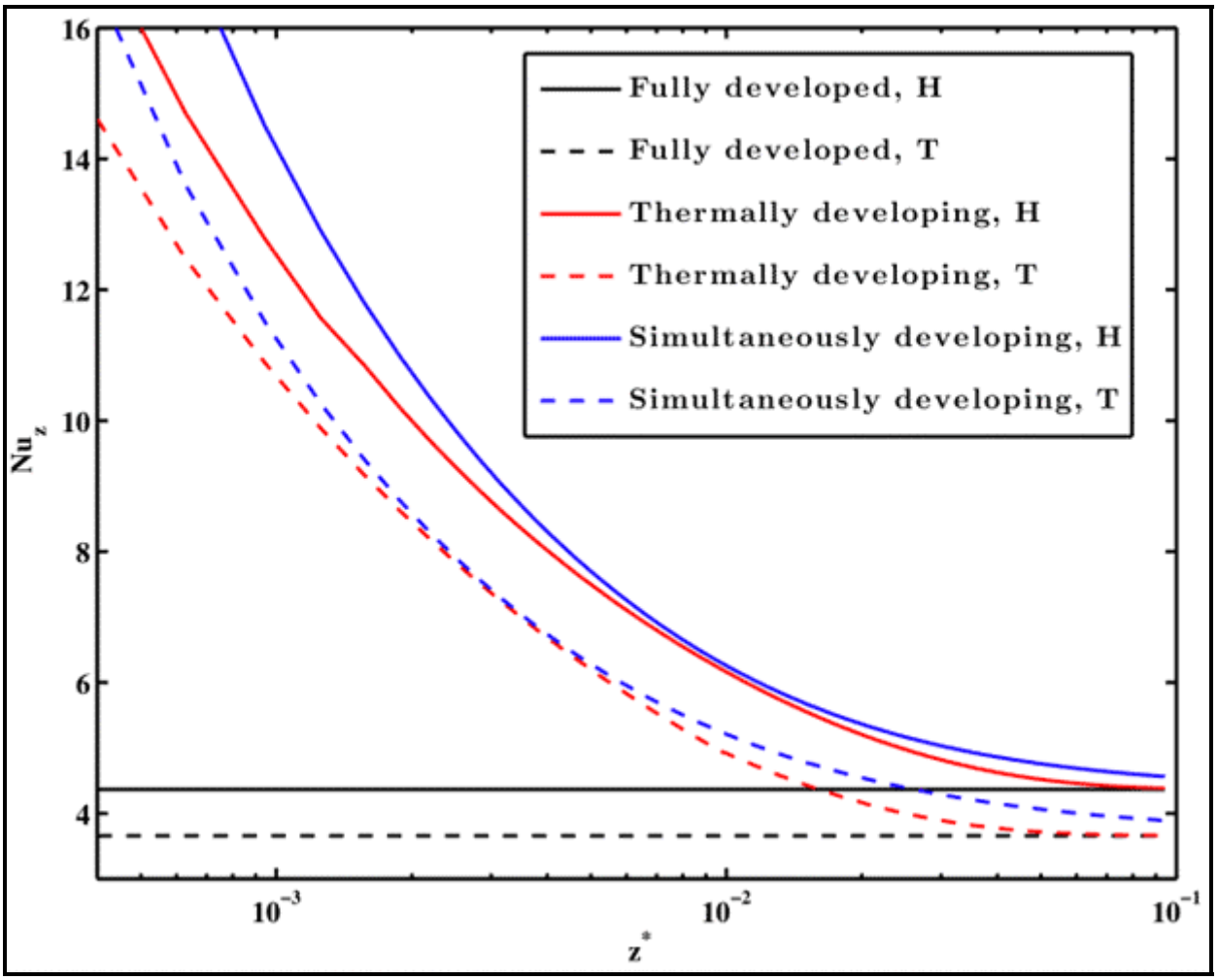

Figure 4.5. Local Nusselt numbers as a function of the dimensionless axial distance z* inside a smooth circular channel for different boundary conditions and flow developments for uniform heat flux (H) and constant wall temperature (T) conditions.

Figure 4.5 shows the heat transfer simulations for single phase flow inside a circular tube for the different boundary conditions and flow developments. The Nusselt numbers in this graph are plotted versus the dimensionless length z* used above, where z* written in terms of the Reynolds and Prandtl numbers is:

$$z^* = \frac{\pi}{4}\left(\frac{z}{Re\,Pr\,d_i}\right) \qquad [4.3.13]$$

This diagram illustrates several important aspects of thermal entry regions. First of all, as the distance from the channel entrance is shortened (while keeping the Reynolds number, Prandtl number and tube diameter constant), the influence of the thermal boundary layer becomes more significant. Secondly, this is also true if the Reynolds number, Prandtl number or channel diameter is increased.

The Hausen (1943) equation is also often cited for the uniform wall temperature boundary condition (T) in a developing laminar flow:

$$Nu_T = \frac{\alpha_{pt}\,d_i}{k} = 3.657 + \frac{0.668\,Re\,Pr(d_i/z)}{1 + 0.04[Re\,Pr(d_i/z)]^{2/3}} \qquad [4.3.14]$$

In this expression, z is the length from the entrance of the tube and it gives the mean Nusselt number up to length z, Nu_T. The older and simpler expression of Seider and Tate (1936) is also often quoted, for a combined entry length for a uniform wall temperature condition (T), that which gives the mean Nusselt number as:

$$Nu_T = \frac{\alpha_{pt}\,d_i}{k} = 1.86\,Gz^{1/3}\left(\mu_{bulk}/\mu_{wall}\right)^{0.14} \qquad [4.3.15]$$

This expression can be used for both heating and cooling conditions and includes the fluid property effects through the bulk to wall viscosity ratio. It is applicable when $0.48 < Pr < 16700$ and $0.0044 < (\mu_{bulk}/\mu_{wall})^{0.14} < 9.75$. Bulk physical properties in the above expressions should be taken at the mean fluid temperature between inlet and outlet.

Gnielinski (1995) proposed a complete set of equations for the mean Nusselt number for laminar, transition and turbulent flows based on a large experimental database. In the laminar regime ($Re < 2300$), the mean value of the Nusselt number up to length z was correlated with the Graetz number for the uniform temperature and uniform heat flux boundary conditions. For the uniform wall temperature condition (T), using the definition of Gz above, Gnielinski (1995) proposed the following asymptotic correlation for the mean Nusselt number Nu_T:

$$Nu_T = \frac{\alpha_{pt}\,d_i}{k} = \left\{Nu_{T,1}^3 + \left[Nu_{T,2} - 0.7\right]^3 + Nu_{T,3}^3\right\}^{1/3} \qquad [4.3.16]$$

The individual values of $Nu_{T,1}$, $Nu_{T,2}$ and $Nu_{T,3}$ are obtained as follows:

$$Nu_{T,1} = 3.66 \qquad [4.3.17a]$$

$$Nu_{T,2} = 1.615\,Gz^{1/3} \qquad [4.3.17b]$$

$$Nu_{T,3} = \left(\frac{2}{1+22\,Pr}\right)^{1/6} Gz^{1/2} \qquad [4.3.17c]$$

For the uniform heat flux boundary condition (H), Gnielinski (1995) proposed two expressions for the mean Nusselt number Nu_H, where the larger of the two values of Nu_H from these expressions is used:

$$Nu_H = \frac{\alpha_{pt}\, d_i}{k} = \left\{Nu_{H,1}^3 + 0.6^3 + \left[Nu_{H,2} - 0.6\right]^3\right\}^{1/3} \qquad [4.3.18a]$$

$$Nu_H = \frac{\alpha_{pt}\, d_i}{k} = 0.924\, Gz^{1/3}\left(Re\frac{d_i}{z}\right)^{1/6} \qquad [4.3.18b]$$

The values of $Nu_{H,1}$ and $Nu_{H,2}$ are obtained as follows:

$$Nu_{H,1} = 4.364 \qquad [4.3.19a]$$

$$Nu_{H,2} = 1.953\, Gz^{1/3} \qquad [4.3.19b]$$

In these expressions at very low Reynolds numbers, each tends to the Nusselt number corresponding to the respective theoretical value for fully developed flow.

For fluid property effects for the other methods, using the recommendations of Lienhard and Lienhard (2006), it is most common to correct these expressions by multiplying the heat transfer coefficient by the ratio of $(\mu_{bulk}/\mu_{wall})^{0.11}$ for heating liquids ($T_{wall} > T_{bulk}$) but $(\mu_{bulk}/\mu_{wall})^{0.25}$ for cooling liquids ($T_{wall} < T_{bulk}$). A single exponent of 0.14 is also found in many textbooks. Instead, for heating of gases the ratio $(T_{bulk}/T_{wall})^{0.47}$ is used while no correction is used when cooling of a gas ($T_{wall} < T_{bulk}$). These terms correct the heat transfer coefficient for the effect of the variation in viscosity between the bulk fluid temperature and that at the tube wall.

The pressure drop in a tube of length L is given by the expression:

$$\Delta p = \frac{2 f \dot{m}^2 L}{\rho d_i} \qquad [4.3.20]$$

For laminar fully developed flow, the following expression can be derived from first principles for the friction factor, adding then the viscosity ratio effect added:

$$f = \left(\frac{16}{Re}\right)\left(\frac{\mu_{bulk}}{\mu_{wall}}\right)^m \qquad [4.3.21]$$

In the study by Marner and Bergles (1985), they recommended a value of m = -0.12 for cooling of a fluid and m = -0.25 when heating a fluid for: circular tubes, internally finned tubes and tubes with twisted tape inserts. For heat transfer in a plain tube, an internally finned tube and a tube with a twisted tape insert, they found the term $(\mu_{bulk}/\mu_{wall})^{0.14}$ worked well for their data for both heating and cooling of liquids, finding however significantly different correlating expressions for the Nusselt number for heating and cooling that are described later in this chapter. These above expressions for heat transfer and pressure

drop, however, do not take into account any effects of natural convection on the flow, which can increase these values by two to three times.

The above expression can also be written for isothermal flows in terms of the Poiseuille number Po as:

$$f\,\mathrm{Re} = \mathrm{Po} = 16 \qquad [4.3.22]$$

This is valid for a circular channel but varies for different channel cross-sectional geometries. For example, the value for a rectangular channel varies from 14.2 to 24, depending on the aspect ratio of the channel, while for an equilateral triangle the value is 13.33 and for an ellipse the value varies from 16 to 19.7, depending on the aspect ratio.

For a developing hydrodynamic boundary layer, the friction factors are higher. From a physical viewpoint, because of the reduction in the fluid velocity near the wall in the developing boundary layer, continuity requires that the fluid in the centre core must accelerate, which in turn thins the boundary layer. Once the opposing boundary layers meet at some distance down the length of the channel, the flow is fully developed. In the entrance region, however, the thinning of the boundary layer and the acceleration of the fluid in the core region give rise to an increase in shear. For a more detailed description, see for example White (1991). This increase in shear is reflected in an increase in pressure drop, which in turn is reflected in an increase in friction factor. This increase is termed the *apparent* friction factor, with Shah and London (1978) giving an interpolation formula for many duct shapes. This is given by

$$f_{\mathrm{app}}\,\mathrm{Re} = \frac{3.44}{\sqrt{\chi}} + \frac{\mathrm{Po} + (\mathrm{K}/4\chi) - \left(3.44/\sqrt{\chi}\right)}{1 + \left(0.000212/\chi^2\right)} \qquad [4.3.23]$$

where $\chi = (z/d_i)/\mathrm{Re}$ and K is the excess pressure drop in the hydrodynamic developed region given by Shah and London (1978) as $K = 1.2 + 38/\mathrm{Re}$. The values of Po in the Poiseuille relation are those mentioned earlier for the various shaped channels. The value of the apparent friction factor is used in place of the usual value to calculate the pressure gradient.

4.4 Laminar Flow and Heat Transfer in Non-Circular Channels

Rectangular channels are an important non-circular shape channel and are characterized by their aspect ratio of 2b/2a, where 2a is the long side and 2b is the short side of the rectangular cross-section. Table 4.1 gives tabular values for a selection of channel shapes and aspect ratios from Shah and London (1978) and Shah and Sekulić (2003) for fully developed laminar flow for the boundary conditions of uniform temperature (T) and two uniform heat flux boundary conditions, where both represent a constant heat flux boundary condition along the channel axis but (H) has a *constant wall temperatur*e around the perimeter of the channel while the other less known boundary condition (HA) has a *constant heat flux* around the perimeter of the channel. Both boundary conditions yield the same Nusselt number for circular channels and parallel plates but they are significantly different for non-circular ducts since the local heat transfer coefficients around the perimeter are not uniform (the perimeter averaged values are reported in Table 4.1). The uniform temperature boundary condition (T) is for when the boundary is everywhere at the same temperature, both axially and around the perimeter of the channel. In the literature, the condition (H) is also referred to as (H1) and (HA) as (H2).

Table 4.1. Heat Transfer and Friction Factors for Fully Developed Laminar Flow in Various Shaped Channels.

Geometry ($z/d_h>100$)	Aspect Ratio (2b/2a)	Nu_H	Nu_{HA}	Nu_T	Po = f Re
Circle	-	4.364	-	3.657	16
Hexagon	-	4.002	3.862	3.340	15.054
Equilateral Triangle	-	3.11	1.892	2.47	13.25
Square	1	3.608	3.091	2.976	14.227
Rectangle	1/2	4.123	3.017	3.391	15.548
	1/4	5.331	2.940	4.439	18.233
	1/6	6.049	2.930	5.137	19.702
	1/8	6.490	2.940	5.597	20.585
Parallel Plates	0	8.235	5.3855	7.541	24

The exact boundary condition around the perimeter of the channel should be considered with care for small channels, viz. the heat transfer coefficient will be large and if the conduction resistance of the tube wall is comparable to the convective resistance within the duct, then temperature or wall heat flux variations around the channel perimeter become significant and thus non-uniform. This will significantly affect the value of the Nusselt number in a laminar flow. As pointed out by Lienhard and Lienhard (2006), rectangular duct values for a uniform wall heat flux, for example, tend to assume a uniform temperature condition around the perimeter of the tube, if the wall has no conduction resistance around its perimeter.

When applying methods to non-circular channels, the Reynolds number is based on the actual mean fluid velocity in the channel's cross-section of area A and the hydraulic diameter is $d_h = 4A/P$, where A is the cross-sectional area of the channel and P is the perimeter of the channel. Note that the mean velocity is *not* calculated with the area that could be determined with the hydraulic diameter.

For laminar fully developed flows in smooth rectangular channels (where an aspect ratio of 2b/2a = 1 for square channels and 2b/2a = 0 for two parallel plates), Shah and Sekulić (2003) give the follow equations for the Nusselt number for the boundary conditions (T), (H) and (HA):

$$Nu_T = \frac{\alpha_{pt}\, d_h}{k} = 7.541\left[\begin{array}{l} 1 - 2.610\left(\frac{2b}{2a}\right) + 4.790\left(\frac{2b}{2a}\right)^2 \\ -5.119\left(\frac{2b}{2a}\right)^3 + 2.702\left(\frac{2b}{2a}\right)^4 \\ -0.548\left(\frac{2b}{2a}\right)^5 \end{array}\right] \qquad [4.4.1]$$

$$Nu_H = \frac{\alpha_{pt}\, d_h}{k} = 8.235\left[\begin{array}{l} 1 - 2.041\left(\frac{2b}{2a}\right) + 3.0853\left(\frac{2b}{2a}\right)^2 \\ - 2.4765\left(\frac{2b}{2a}\right)^3 + 1.0578\left(\frac{2b}{2a}\right)^4 \\ - 0.1861\left(\frac{2b}{2a}\right)^5 \end{array}\right] \qquad [4.4.2]$$

$$Nu_{HA} = \frac{\alpha_{pt}\, d_h}{k} = 8.235\left[\begin{array}{l} 1 - 10.6044\left(\frac{2b}{2a}\right) + 61.1755\left(\frac{2b}{2a}\right)^2 \\ - 155.1803\left(\frac{2b}{2a}\right)^3 + 176.9203\left(\frac{2b}{2a}\right)^4 \\ - 72.9236\left(\frac{2b}{2a}\right)^5 \end{array}\right] \qquad [4.4.3]$$

Note that for (2b/2a) = 0, the above expressions give the fully developed flow values corresponding to two parallel plates. They apply when the heat is transferred from all sides of the rectangular channel. When one or more sides is/are adiabatic, the special rules apply…see there publication for details.

Shah and London (1978) tabulated the numerical results from Wibulswas (1966) as a function of the Graetz number in terms of z* and the aspect ratio for handling of entrance region effects. For design purposes, the local perimeter averaged Nusselt values were put in terms of a Taylor series expansion for the uniform heat flux boundary condition (H), given by:

$$Nu_{H,z} = \frac{\alpha_{pt}\, d_h}{k} = 3.04 + \frac{0.0244}{z^*} + \frac{0.448}{(2b/2a)} - \frac{0.0000269}{(z^*)^2} + \frac{0.02}{(2b/2a)^2} - \frac{0.000678}{z^*(2b/2a)} \qquad [4.4.4]$$

$$z^* = \frac{\pi}{4}\left(\frac{z}{Re\, Pr\, d_h}\right) \qquad [4.4.5]$$

The ratio (2b/2a) is the aspect ratio of the channel (2a = width and 2b = height) and is valid when $0.05 \le z^* \le 0.2$ and $0.25 \le (2b/2a) \le 1.0$. In this expression, the hydraulic diameter is d_h. This expression is shown graphically in Figure 4.6. It predicts tabular values for rectangular channels with deviations of less than 2%. The method is based on the assumption that axial heat conduction, viscous dissipation and thermal energy sources within the fluid are negligible. A similar relationship was developed for a (T) boundary condition obtained from tabulated data of Wibulswas (1966), given as

$$Nu_{T,z} = \frac{\alpha_{pt}\, d_h}{k} = 2.117 + \frac{0.01667}{z^*} + \frac{0.6713}{(2b/2a)} - \frac{0.00001136}{(z^*)^2} + \frac{0.02835}{(2b/2a)^2} - \frac{0.000886}{z^*(2b/2a)} \qquad [4.4.6]$$

This is valid when $0.05 \le z^* \le 0.2$ and $1/6 \le (2b/2a) \le 1.0$.

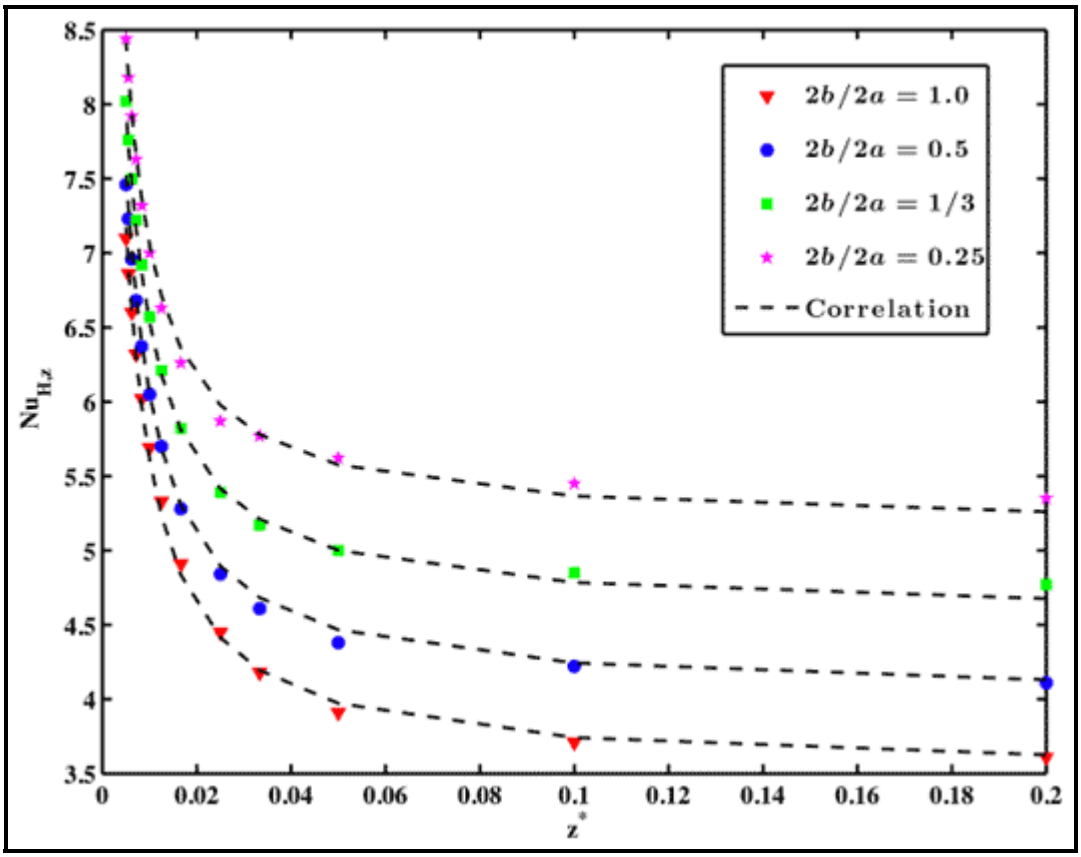

Figure 4.6. Local Nusselt number expression for the (H) boundary condition compared to tabulated data plotted versus non-dimensional length from entrance for rectangular channels of various aspect ratios.

For friction factors in rectangular channels, Wei and Joshi (2004) proposed the following expression for the apparent friction factor for laminar developing flows where $\chi = (z/d_h)/Re$:

$$f_{app}\, Re = \left[\frac{3.44}{\sqrt{\chi}} + \frac{24 + (0.674/\chi) - (3.44/\sqrt{\chi})}{1 + (0.000029/\chi^2)}\right] F_{aspect} \qquad [4.4.7]$$

F_{aspect} is the aspect ratio correction factor, calculated from their polynomial expression:

$$F_{aspect} = 1 - 1.3553\left(\frac{2b}{2a}\right) + 1.9467\left(\frac{2b}{2a}\right)^2 - 1.7012\left(\frac{2b}{2a}\right)^3 + 0.9564\left(\frac{2b}{2a}\right)^4 - 0.2537\left(\frac{2b}{2a}\right)^5 \quad [4.4.8]$$

Another important method for predicting the friction factors and Nusselt numbers in the combined entrance region of non-circular ducts and channels (providing both local and average Nusselt numbers) is proposed by Muzychka and Yovanovich (2004). Their method is applicable to both isothermal (T) and iso-heat flux (H) boundary conditions and for a wide range of channel shapes. The reader is referred to their publication for details.

Various prediction methods are available for special microscale flow geometries. For example, Colgan et al. (2007) have tested water for interrupted microfin channel arrays and correlated the heat transfer and pressure drop results. For micro-pin-fin geometries, one is referred to the work of Brunschwiler et al. (2008) for tests with water and propositions for predicting pressure drops and heat transfer.

4.5 Special Effects on Laminar Flow and Heat Transfer in Microchannels

No new governing equations are required for laminar flow heat transfer in microchannels (channels less than ~1 mm) as noted by Morini (2008) in his detailed review on this subject, but the relative weight of the different terms in the momentum and energy equations can be very different when going from macroscale to microscale. Furthermore, he states that no natural or mixed convection are evidenced in the laminar regime in microchannels, even for large temperature differences between the fluid and the heated walls. According to Morini (2008), the first study on microscale flow was that of Poiseuille (1840), who tested channels having an internal diameter down to 15 microns in order to analyse the law of the mass flow rate in capillary tubes using water. These experimental data obtained by Poiseuille in 1840 were used to state the famous "Poiseuille law" for laminar flows through circular tubes, according to which the product of the friction factor times the Reynolds number is a constant (f Re = 16 = Po for circular tubes).

For the most part, laminar flow and heat transfer in microchannels is well described by the classical laminar flow theory above. However, special aspects can become significant in microchannels that were only of minor influence in larger channels. The smaller the diameter becomes, the more the behavior tends to deviate from the theoretical values derived for macro-channels. These behaviors have been observed by Tiselj et al. (2004), Celata et al. (2006a), Celata et al. (2006b), to name but a few. However, these deviations tend to only become evident as the channel size becomes very small.

As mentioned above, some effects neglected in macroscale flow become important in microscale flow. The reduction in the size of channels to the microscale can introduce some *scaling effects* and *micro-effects*, using the classification proposed by Herwig and Hausner (2003), who noted that it is important to distinguish between these two concepts. First of all, according to their analysis, *scaling effects* are those which may be neglected at the referenced geometrical scale, but which become important when the scale changes, e.g. the reduction of the channel diameter implies a larger reduction in its volume than in its internal surface area, so that the area-to-volume ratio tends to be very high as the channel size is reduced. This implies a prevalence of surface forces over body forces, such that the advection terms in the conservation equations prevail over those related to volume forces. Owing to this, microscale flow behavior can differ remarkably from macroscale channel flow. Secondly, *micro-effects* are those which

require a reformulation of the conservation equations and/or their associated boundary conditions as the characteristic scale of the system is reduced, e.g. this is confronted when the molecular mean free path of a gas flow becomes the same order of magnitude as the diameter of the channel, so that the fluid cannot be treated as a continuous phase and the Navier-Stokes equations are no longer appropriate for modeling the flow.

According to Morini (2006, 2008), the most important scaling effects are as follows in order of importance:

- Viscous dissipation (causes heating of the fluid);
- Conjugate effects (such as axial conduction along the channel walls);
- Thermal entrance effects (although this can be important in macrochannel flows as well).

Initially, neglecting these effects, numerous experimental papers concluded that the classical laminar flow theory did not work well for microchannels. However, this was shown by the above mentioned studies not to be true. For example, all the experimental runs of Celata et al. (2008) are in agreement with the classical methods for pure forced convection within the experimental uncertainty. This indicates that it is possible to use conventional methods for convective heat transfer coefficients in microchannels as long as the role of the main scaling effects (like viscous dissipation, conjugate heat transfer and so on) can be considered negligible (this should be verified on a case-by-case basis and not loosely assumed to be the situation in engineering applications). In fact, the classical methods do work but have to be supplemented by additional attention to details, such as the accurate measurement of the internal diameter of the channel, the "roundness" and uniformity of the cross-sectional profile of a circular channel, the internal roughness, including viscous heating in the energy balance, etc.

With particular respect to surface roughness of the interior of microchannels, Celata et al. (2008) observed no effect of the relative roughness (the ratio of the roughness to diameter), when it was below 4%, on the average Nusselt number in their laminar experimental tests. On the contrary, the tests of Kandlikar, Joshi and Tian (2001) demonstrated evidence of a strong effect of relative roughness on the Nusselt number in the laminar regime, even for relative roughnesses less than 2%. Therefore, the threshold of the effect of relative roughness seems to require more study and confirmation of when it becomes influential, besides any effect of the topology of the roughness.

The principal scaling effects noted above plus physical property effects are discussed in the subsections below. For readers interested in a more detailed discussion on single-phase microscale flows, they are referred to the book of Kandlikar and Garimella (2005) and the review of Morini (2008).

4.5.1 Viscous Heat Dissipation

It is common in macroscale theoretical developments to ignore the viscous heating term in the energy equation. In the microscale, this term can become important. According to Morini (2006), the bulk temperature difference between the inlet and outlet of a microchannel can be viewed as the sum of the temperature rise of the fluid due to the heat flux at the walls ΔT_q and the temperature rise of the fluid due to viscous heat dissipation ΔT_{visc}. This is mathematically given by

$$\Delta T_{bulk} = \Delta T_q + \Delta T_{visc} \qquad [4.5.1]$$

It was shown that the temperature rise due to viscous heat dissipation ΔT_{visc} is a function of the Reynolds number Re, the channel diameter d_i (or the hydraulic diameter d_h), length of the microchannel L (or the distance from the entrance z), and the Poiseuille number Po = fRe. This is given by

$$\Delta T_{visc} = 2\,Re\left(\frac{\nu^2}{c_p}\right)\left(\frac{Po\,L}{d_i^3}\right) \qquad [4.5.2]$$

The temperature rise increases with the square of the kinematic viscosity ν and inversely to the cube of the channel diameter d_i. For an adiabatic channel wall condition, the temperature rise due to viscous heat dissipation can be put into a dimensionless form as

$$\frac{\Delta T_{visc}}{\Delta T_{ref}} = 4\left(\frac{Ec}{Re}\right)\left(\frac{Po\,L}{d_i}\right) \qquad [4.5.3]$$

Here, Ec is the Eckert number, which is given as

$$Ec = \frac{(\dot{m}/\rho)^2}{2c_p\Delta T_{ref}} \qquad [4.5.4]$$

The top term on the right gives the mean velocity of the fluid. Po is the Poiseuille number, which is also given as (f Re). For laminar flow, this value is normally constant, depending on the shape of channel and its aspect ratio, as discussed earlier. The reference temperature rise ΔT_{ref} can, as suggested by Morini (2006), be chosen as the value for which the dynamic viscosity of the fluid decreases by approximately 2-3%. Thus, for an adiabatic channel, the limit to which viscous heat dissipation can be neglected is when the temperature rise is less than the reference temperature difference ΔT_{ref} in the above expression. This limit is given as:

$$4\left(\frac{Ec}{Re}\right)\left(\frac{Po\,L}{d_i}\right) < 1 \qquad [4.5.5]$$

Thus, the limiting Reynolds number where viscous dissipation cannot be neglected is when

$$Re > \frac{1}{2}\left(\frac{c_p}{\nu^2}\right)\frac{d_i^3}{L\,Po}\Delta T_{ref} \qquad [4.5.6]$$

The above expression highlights the fact that when the internal diameter decreases, the limiting Reynolds number for which the viscous dissipation cannot be ignored tends to decrease.

For a heated channel, Morini (2006) showed that κ, the ratio of the temperature rise due to viscous heating to the temperature rise related to the heat flux at the walls, can be given by:

$$\kappa = \frac{\Delta T_{visc}}{\Delta T_q} = \frac{2Br\,Po\,A}{d_i} \qquad [4.5.7]$$

In this expression A is the channel cross-sectional area, i.e. for a circular channel $A/d_i^2 = \pi/4$.

The Brinkman number Br is given in terms of the dynamic viscosity, the heat flux at the wall q and the mean fluid velocity calculated from the mass flux and density as:

$$Br = \frac{\mu(\dot{m}/\rho)^2}{q} \qquad [4.5.8]$$

Setting a limit on the temperature ratio κ_{lim} gives the upper bound of when viscous heat dissipation can be neglected. Thus, this is when

$$Br < \frac{\kappa_{lim}}{2A/(d_i^2\, Po)} \qquad [4.5.9]$$

This can be put in terms of the Reynolds number for a circular channel as follows:

$$Re < \frac{2\kappa_{lim}\, q}{\pi\, Po} \frac{d_i\, \rho}{\mu^2(\dot{m}/\rho)} \qquad [4.5.10]$$

The limit set on the temperature ratio is suggested to be around 5% or $\kappa_{lim} = 0.05$. Therefore, an easy to implement criterion has been proposed by Morini (2006) for identifying those occasions when viscous heat effects are expected to be notable.

The effect of viscous dissipation may influence the fully developed Nusselt number due to the increase in the Reynolds number, implying an increase in the Brinkman number. Morini (2006) recommends the use of the following equation to obtain the fully developed Nusselt number that includes the effect of viscous heat dissipation $Nu_{H,visc}$ for the uniform heat flux boundary condition (H):

$$Nu_{H,visc} = \frac{Nu_H}{1+\sigma\, Br} \qquad [4.5.11]$$

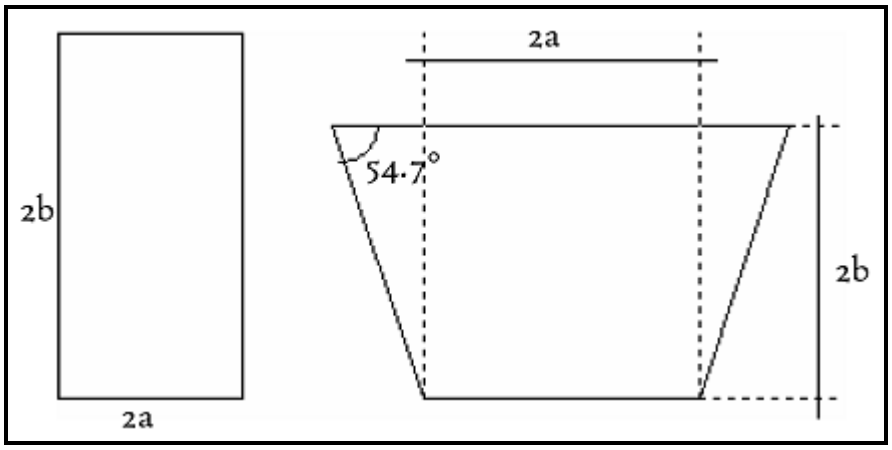

Figure 4.7. Typical microchannel cross-sections obtained by chemical etching on <110> and <100> silicon wafers.

Morini (2006) provided a list of values for Nu_H and σ for different aspect ratios of rectangular microchannels, reproduced here in Table 4.2. As a reference, for a circular microchannel $Nu_H = 48/11$ and $\sigma = 48\pi/11$. Other papers by Morini (2005) and Morini and Spiga (2007) can be consulted on this topic of viscous heating. In Table 4.2, the values of Nu_H and σ are given for rectangular and trapezoidal cross-

sections. The trapezoidal cross section is very common in microfluidics when the microchannels are made from silicon wafers with a photolithographic based process. In this case one can obtain microchannels having a cross-section fixed by the orientation of the wafer crystal planes; for example, the microchannels etched in <110> or <100> silicon wafers have respectively a rectangular or trapezoidal cross-section with an apex angle of 54.7° imposed by the crystallographic morphology of the silicon, as illustrated in Figure 4.7 where the values of 2b and 2a are defined for these two shapes.

Table 4.2. NuH and σ for various aspect ratios for rectangular and trapezoidal channels of Morini (2006).

Aspect Ratio	Rectangle		Trapezoid	
2b/2a	Nu_H	σ	Nu_H	σ
0	8.235	-	8.235	-
0.05	7.451	131.35	7.302	136.51
0.1	6.785	67.98	6.575	73.17
0.2	5.738	36.57	5.536	41.79
0.3	4.990	26.39	4.852	31.58
0.4	4.472	21.57	4.391	26.68
0.5	4.123	18.91	4.073	23.88
0.6	3.895	17.36	3.850	22.14
0.7	3.750	16.42	3.691	20.98
0.8	3.664	15.89	3.577	20.19
0.9	3.620	15.62	3.493	19.62
1.0	3.608	15.54	3.431	19.22
1.25	3.664	15.89	3.338	18.63
1.67	3.895	17.36	3.277	18.28
2.0	4.123	18.91	3.261	18.22
3.33	4.990	26.39	5.251	18.44
5.0	5.738	36.57	3.236	18.70
10	6.789	67.98	3.188	18.99
∞	8.235	-	3.093	19.15

4.5.2. Wall-to-Fluid Conjugate Effects

Conjugate effects become important when the heat transfer due to axial conduction along the channel wall starts to compete with the convective heat transfer from the wall to the fluid. This happens when the laminar heat transfer coefficient is small and the thermal conductivity of the channel wall is high relative to that of the fluid. The result is a deviation in the axial boundary condition from that expected, which in turn influences the laminar convection heat transfer coefficient. This interaction between the convective heat transfer process, the axial conduction process and the boundary condition is referred to as a conjugate effect.

Mori, Sakakibara and Tanimoto (1974) performed a study on circular tubes with respect to the effect of the wall-to-fluid thermal conductivity ratio and the wall thickness on conduction along the tube wall. It was found that for a relatively high thermal conductivity ratio, (k_{wall}/k_{fluid}), if a uniform wall heat flux boundary is imposed, then the temperature distribution at the wall-fluid interface along the channel tends towards a constant value. The same result was found when increasing the ratio of the thickness of the wall to the length of the tube. The greater this ratio becomes, the more uniform the temperature along the tube at the wall-fluid interface tends to become, i.e. the high rate of axial conduction along the tube wall levels

out the axial temperature distribution. Thus, laminar flow solutions for an imposed uniform heat flux boundary condition, such as the solutions presented earlier in this chapter, will approach instead the solution for a constant wall temperature boundary.

The opposite is true for an imposed constant wall temperature boundary. In this case, the thicker the walls the more the solution approaches the uniform heat flux solution. This is because a thick wall has a higher radial thermal resistance, which allows the temperature gradient to develop on the inside wall in the axial direction, as pointed out by Shah and London (1978).

These axial conduction results may have serious implications with regard to determining local heat transfer coefficients of an experimental test section or on the thermal design of a micro-cooling system. In particular, for a channel with a uniform heat flux boundary condition, it is assumed that the bulk fluid temperature distribution from inlet to outlet is linear. However, if the tube wall is thick enough and the ratio of the wall to fluid thermal conductivity is high, then the imposed boundary is in fact closer to that of a constant wall temperature, for which the bulk temperature variation changes exponentially from inlet to outlet, not linearly. Thus, one must be careful when calculating the heat duty using a log mean temperature difference, for example, or even when using local calculations since the temperature profile of the bulk liquid is not that which would otherwise be expected.

These above observations by Mori, Sakakibara and Tanimoto (1974) were made for Graetz numbers equal to 50. From their study, it was shown that for an imposed uniform heat flux boundary, as the Graetz number increases, the conjugate problem approaches the uniform heat flux solution, while as it decreases it approaches the constant wall temperature solution. Based on analysis, for an imposed uniform heat flux boundary condition, the wall may be considered thin if $t_{wall}/L < 0.0001$ for $R_{wall} \approx 2\times10^{-7}$ and when $t_{wall}/L < 0.001$ for $R_{wall} > 10^{-5}$ in Shah and London (1978), where t_{wall}/L is the ratio of the wall thickness to the channel length and R_{wall} is the wall thermal resistance in (K/W). For an imposed constant temperature boundary, the wall may be considered thin if $R_{wall} < 0.01$.

Morini (2008) gives a criterion for when conjugate effects become important, in particular one must pay attention when $Re < 200$. This was based on his theoretical work and that performed by Peterson (1999) and Maranzana, Perry and Maillet (2004). His criterion for circular channels is given as

$$\left(\frac{k_{wall}}{k_{fluid}}\right)\left(\frac{D-d_i}{d_i z}\right)\frac{1}{Re\,Pr} > 0.01 \qquad [4.5.12]$$

In this expression, D is the outside diameter of the channel of internal diameter d_i and k_{wall} is the thermal conductivity of the channel material. Then the term on the left is larger than 0.01, then conjugate effects become important and one must go to appropriate solution methods (beyond the scope of the present review here). For rectangular channels, his expression becomes:

$$\left(\frac{k_{wall}}{k_{fluid}}\right)\left(\frac{d_h}{L}\right)\left(\frac{(L_y)(L_x)}{(2a)(2b)}-1\right)\frac{1}{Re\,Pr} > 0.01 \qquad [4.5.13]$$

In this expression, L_x and L_y are the width and height of the outside of the rectangular microchannel whose internal channel dimensions are 2a and 2b, respectively, as illustrated in Figure 4.8. Thus, the upper bound of Reynolds numbers, that is Reynolds numbers up to where conjugated effects are important, can be determined from the above expression, or from its rearrangement:

$$\mathrm{Re} < \left(\frac{k_{wall}}{k_{fluid}}\right)\left(\frac{d_h}{L}\right)\left(\frac{(L_y)(L_x)}{(2a)(2b)} - 1\right)\frac{100}{\mathrm{Pr}} \qquad [4.5.14]$$

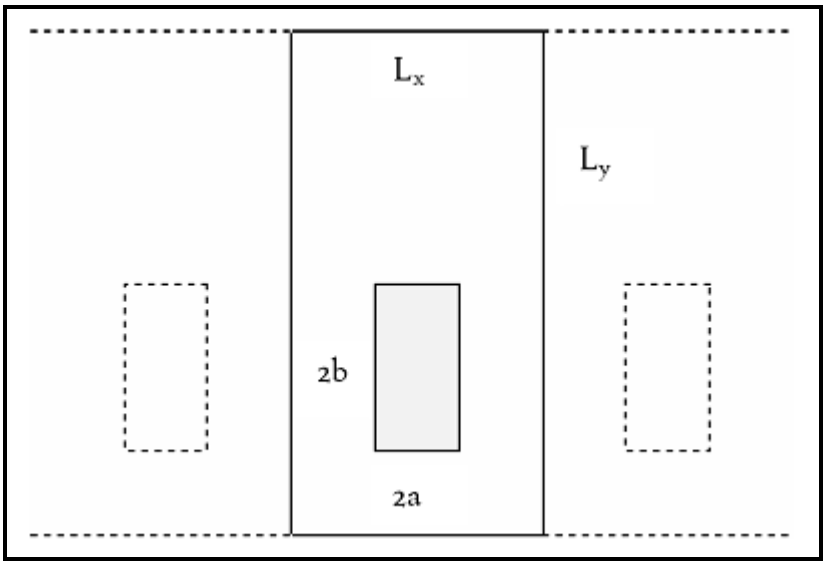

Figure 4.8. Diagram of rectangular microchannel.

4.5.3. Entrance Region Effects

Thermal entrance effects may play an important role inside micro-channels. For a fluid entering a channel at a uniform temperature, the temperature profile starts to develop as it moves along the axial length of the channel. The Nusselt numbers in this thermally developing region are much higher than for fully developed flow, due to the thin thermal boundary layer in this region. Thermal entrance effects also become more pronounced as the Reynolds number increases. For thermally developing flow inside a circular tube with a uniform heat flux boundary, the method proposed earlier in this chapter can be used for local values of the Nusselt number. For length-averaged values of heat transfer coefficient, Morini (2006) suggests the use of the Hausen (1943) correlation format:

$$\mathrm{Nu} = \mathrm{Nu}_H + K_1\frac{\mathrm{Gz}}{1 + K_2\mathrm{Gz}^b} \qquad [4.5.15]$$

where Nu_H is the fully developed value for the particular channel shape using the (T) and (H) boundary conditions. The values of the constants, K1, K2 and b for a circular channel are given in Table 4.3. For a rectangular micro-channel with all four sides heated equally, these values become 0.14, 0.05 and 2/3, respectively. Entrance effects in general can be neglected for Graetz numbers less than 10.

Experimental data are available for only a few limited cases, for example for square channels and parallel plates. Overall, the Nusselt numbers are slightly higher in the entrance region when compared to the thermally developing flow case. Such results may often neglect viscous heat dissipation and axial conduction effects. Most results are obtained by performing a numerical analysis from which the viscous dissipation term's variable property effects are included in the Navier-Stokes equations.

Table 4.3. Constants for circular channels using the expression of Morini (2006).

Wall Condition	Velocity Profile	Pr	Nu	Nu_H	K_1	K_2	b
(T)	Fully dev.	Any	Avg.	3.66	0.0668	0.04	0.66
(T)	Fully dev.	0.7	Avg.	3.66	0.104	0.016	0.8
(H)	Fully dev.	Any	Local	4.36	0.023	0.0012	1
(H)	Fully dev.	0.7	Local	4.36	0.036	0.0011	1

4.5.4. Temperature Gradient Property Effects

As Mahulikar and Herwig (2006) demonstrated theoretically for incompressible laminar microconvective flows at low Reynolds numbers and high heat fluxes, there is an increase in the radial and axial gradients of the fluid properties, which means that the variation of the fluid thermal properties with temperature has to be taken into account in the evaluation of the convective heat transfer coefficients. The two foremost properties that can influence the convective behavior of a fluid in a microchannel were identified to be the viscosity and the thermal conductivity. With respect to the first property, the viscosity variation significantly distorts the axial velocity profile and this distortion varies along the channel, thereby inducing a radial flow due the necessity to maintain continuity of the flow. Mahulikar and Herwig (2006) in fact demonstrated that the resulting induced radial heat convection can be a significant percentage of the axial heat convection, especially in microchannels. Also, axial conduction is induced to the fluid by the variation of the thermal conductivity along the flow. The effects of the distortion in the axial velocity profile and the induced radial flow due to fluid viscosity variation are in opposition to one another. However, the axial and radial variations in the thermal conductivity in the flow have a superimposing effect on the microconvection process. Consequently, at low Reynolds numbers ($Re < 10$), the average Nusselt number becomes dependent on the fluid average temperature and on the heat flux imposed at the wall, which is contrary to the normal basic premise of laminar convection being heat flux independent.

4.6 Mechanisms of Laminar Heat Transfer Augmentation

Extended Surface Area. One way to increase laminar heat transfer coefficients is to increase the surface area in contact with the fluid to be heated or cooled. It is most common to develop heat transfer correlations for internal flows in enhanced tubes based on the internal ***nominal*** surface area, i.e. that of the perimeter of the maximum internal diameter of the tube d_i (corrugations) or at the base of any internal enhancement (fins or ribs) [***all correlations in this chapter follow this format***]. This heat transfer coefficient is that which can be used directly in calculating the overall heat transfer coefficient at this diameter without use of a surface area ratio. It is *not* common practice to reduce single-phase flow heat transfer data relative to the total internal surface area. On the other hand, if internal fin efficiency becomes important, it is not possible to include this effect in nominal internal area based correlations. However, commonly used fins and ribs are quite small and their fin efficiencies are normally over 0.95 while for copper tubes they approach 0.99. Since the original experimental data would normally have been reduced to a heat transfer correlation without correcting for fin efficiency, this effect is already incorporated for tubes of that same material. Thus, an effect of fin efficiency can normally be safely ignored. On the other hand, twisted tape inserts fit rather loosely inside a tube (thus they have poor thermal contact to the inner tube wall but can be easily installed and removed) and hence the surface area of a twisted tape is not considered to be heat transfer surface area, only that of the plain tube perimeter in which it is installed. Furthermore, any tube surface area blocked by the width of the insert adjacent to the tube wall is still usually considered to be effective heat transfer area.

Surface Roughness. The internal roughness of the tube surface is well known to increase the turbulent heat transfer coefficient but usually has little or no effect on laminar heat transfer, except in extreme cases such as very small channel sizes.

Swirl. Swirl of the flow is known to augment heat transfer. Large internal helical fins or ribs, corrugations and twisted tapes impart a swirl effect on the fluid. This tends to increase the effective flow length of the fluid through the tube, which increases heat transfer and pressure drop. For twisted tape inserts, the effect of swirl on augmentation plays an important role. With regard to small fins or corrugations, they are often not sufficient to create a swirl effect and hence may not offer any or much in the way of enhancement.

Laminar Flow Displacement. The displacement of the laminar flow from the heat transfer wall is a particularly important heat transfer mechanism for augmenting heat transfer. This is for instance done by placing a twisted tape in the path of the flow that forces the flow away from the wall and allows fresh bulk fluid to come into contact with the wall.

4.7 Laminar Heat Transfer with Twisted Tape Inserts

A schematic diagram of a twisted tape insert inside a tube is shown in Figure 4.9. The enhancement is defined geometrically by the thickness of the tape δ and its twist ratio, y. The twist ratio is defined as the axial length for a *180°* turn of the tape divided by the internal diameter of the tube. ***This is the most common definition used in research literature and that used here***. It is also common to use the axial length for a complete *360°* turn to calculate the twist ratio; hence, one must double-check the definition used before applying a twisted tape prediction method or using experimental results from manufacturer's literature or a scientific publication and then make sure to indicate the definition used in the resulting heat exchanger specification sheet when specifying a twisted tape insert. An excellent overview of laminar flow twisted tape research over the years is available in Manglik and Bergles (1992a). For treatment of turbulent flow and heat transfer with twist tape inserts, refer to Chapter 5 in this book.

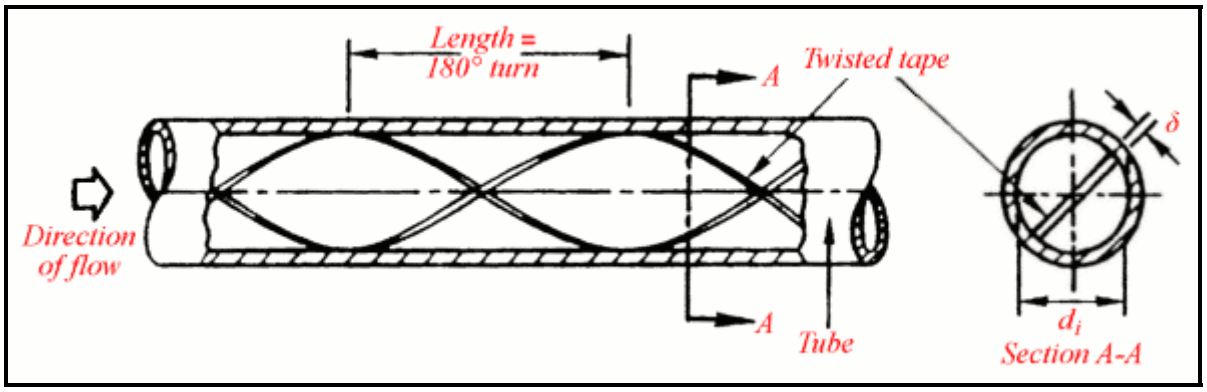

Figure 4.9. Diagram of a twisted tape insert inside a tube.

A twisted tape insert tends to sit loosely within a tube without making "thermal" contact with the tube wall and hence the surface area of the twisted tape itself is not taken into consideration for heat transfer purposes, instead only its effect on the heat transfer coefficient of the tube's inner surface. The reason that a tight fit is not usually possible is that heat exchanger tubing has tolerances on the tube diameter and wall thickness; hence, when specifying the diameter of the twisted tape, these tolerances must be taken into consideration to make sure the tape will fit into the tube. Furthermore, this means that the tape must be held in place using some type of "hook" at the entrance of the tubesheet to prevent the tape from being pushed downstream by the pressure drop. For cleaning purposes, twisted-tapes can be removed and tend

to bring some of the fouling layer with them; however, the force to remove the tapes that are stuck in the tubes may extend them and require a fresh set of tapes be ready for installation.

Since twisted tapes can be installed in existing heat exchangers (as well as in new heat exchangers), they are often a cost-effective solution for increasing the thermal capacity compared to the installation of a new larger heat exchanger and the associate piping and foundation changes for its installation. On the other hand, the larger pressure drop imposed by the twisted-tape may require the number of tube passes in the heat exchanger to be reduced but normally the thermal performance is still considerably increased. For even higher thermal performance that a twisted-tape insert, one should consider the use of the wire mesh inserts of Cal Gavin Ltd. that have been very successfully applied to enhance many laminar flow services (refer to their manufacturer for details and thermal performance). Below, a summary of the limited number of experimental studies on laminar flow heat transfer with twisted-tape inserts is presented and several methods for predicting their heat transfer and pressure drop characteristics.

Apparently, the first comprehensive study on twisted tape heat transfer in laminar flows was presented in a series of papers by Date and Singham (1972), Date (1973) and Date (1974), in which the uniform heat flux boundary condition (H) was investigated numerically and both heat transfer and pressure drop simulations were reported. The flow conditions were idealized for a zero tape thickness but the twist of the tape and heat conduction effects in the tape (as if it were a fin) were included. Shortly after, Hong and Bergles (1976) presented experimental results for water and ethylene glycol in an electrically-heated tube for this boundary condition that demonstrated heat transfer augmentation ratios as high as ten compared to a plain tube, illustrating the very high potential of twisted tape inserts for enhancing laminar flows. They also presented a preliminary heat transfer correlation. DuPlessis (1982) and DuPlessis and Kröger (1983) next made twisted tape measurements for heating and cooling of SAE 20 lubricating oil and presented a method to describe their data. Furthermore, Watanabe, Taira and Mori (1983) experimentally investigated twisted tape inserts for high temperature applications and proposed heat transfer and friction factor correlations.

Marner and Bergles (1978) reported the first heat transfer data for laminar flow of a viscous liquid (ethylene glycol) in tubes with twisted-tape inserts for the uniform wall temperature (T) boundary condition, using condensing steam as the heating fluid. They observed heat transfer augmentations up to three times that of a plain tube. Subsequently, Marner and Bergles (1985) extended this experimental study for a 23.0 mm internal diameter, 2.44 m length tube with a twisted tape insert of 22.9 mm diameter, a tape thickness of 1.22 mm and a twist ratio of 5.4. The tests were done with Polybutene 20 and the test conditions were for essentially a constant wall temperature boundary condition when using steam condensation in the annulus of a double-pipe heat exchanger for heating the test fluid but were probably closer to constant heat flux conditions when cooling the test fluid using a counter-current flow of water in the annulus. In isothermal pressure drop tests, they found a Poiseuille number of 54 (Po = f Re = 54) compared to Po = 16 for the same tube without the insert, indicating a pressure drop penalty ratio of 3.4 for this particular twisted tape. For viscosity ratio ranges from 7.37 to 33.3 for heating and 0.00464 to 0.0469 for cooling, the twisted tape Nusselt numbers were from 1.5 to 2.25 times those of the plain tube at equivalent Graetz numbers. In contrast to the internally finned tube tested in the same study, they found about the same amount of enhancement for both heating and cooling when using the twisted tape. They explained this as being a sort of "scraping" process of the fluid from the wall of the tube and its replenishment by bulk liquid from the center of the tube. They were able to correlate all their data for both heating and cooling of the test fluid using the following correlation:

$$Nu_{T,tt} = \frac{\alpha_{tt} d_i}{k} = 1.322 Gz^{0.458} \left(\frac{\mu_{bulk}}{\mu_{wall}} \right)^{0.14} \qquad [4.7.1]$$

This expression includes the Graetz number, which is defined as:

$$Gz = \left(\frac{\pi}{4}\right)\frac{Re\,Pr\,d_i}{L} \qquad [4.7.2]$$

Most of the data were predicted to within 20% by this expression for this one twisted tape ratio for their tests covering Reynolds numbers from 15.1 to 575, Prandtl numbers from 1260 to 8130 and Graetz numbers from 868 to 6570 for the above mentioned viscosity ratio range. Entrance length effects are thus included within this correlation as the database was for the mean heat transfer coefficients along the entire tube. From the diabatic pressure drop tests, they recommended different viscosity ratio corrections, mentioned earlier in this chapter in Section 4.3.

Monheit (1987) performed an experimental study on a 21.6 mm internal diameter, 6.7 m length tube with a twisted tape insert of 21.2 mm width before twisting, a tape thickness of 1.0 mm and twist ratios of 2.0, 2.8 and 3.7. The tests were done for cooling of synthetic lubricating oil (Shell turbo-oil 68) in a tube with twisted tape inserts in a double-pipe heat exchanger with water as the cooling fluid, whose experimental boundary condition is probably close to a constant heat flux condition under fully developed flow conditions. Absolute values of the friction factors and Nusselt numbers measured were not however given; all data were presented as ratios with respect to the tape with y = 2.8 at a Reynolds number of 500. In any case, it was found that the y = 2.0 tape outperformed the reference tape by about 20-25% while the y = 3.7 tape performed about 10-15% less than the reference tape. With respect to the pressure drops, the y = 2.0 tape had about 30-40% higher-pressure drops while the y = 3.7 tape had about 16-18% lower ones. In addition to the plain tapes, one twisted tape with punched holes with y = 2.8 and another tape with slit edges with y = 7.0 were tested. No improvement in heat transfer with respect to the y = 2.8 plain tape was found with the punched holes and lower heat transfer performance was found with the larger twist ratio of 7.0. No prediction method was proposed here however.

Manglik and Bergles (1986) numerically examined the special case of a tape insert without twist (that is a straight tape with $y = \infty$) and negligible thickness. The flow is thus in a semi-circular channel. Constant physical properties were assumed. Two numerical cases were examined: (i) uniform axial heat flux and constant circumferential tube wall temperature (H) and (ii) constant axial and circular arc section tube wall temperature (T). These two conditions they noted essentially form the two extremes of the fin effect of a twisted tape insert, with the second case defining the lower idealized limit. They pointed out that loose fitting tapes used in experiments and industrial practice correspond to a condition in-between these two cases. In particular, for the semi-circular channel they determined the fully developed Nusselt number for case (T) to be $Nu_T = 4.631$ relative to the value of $Nu_T = 3.657$ for the circular tube geometry, i.e. 26.6% higher for a straight insert. Following this work, Manglik and Bergles (1987) proposed a new generalized twisted tape heat transfer correlation based on the twist ratio y.

Saha, Gaitonde and Date (1989) investigated the heat transfer and pressure drop characteristics of laminar flow in a tube with regularly spaced twisted tape segments, looking for ways to reduce pressure drop while maximizing heat transfer. Furthermore, Bandyopadhyay, Gaitonde and Sukhatme (1991) studied the influence of natural convection on heat transfer during laminar flow in tubes with twisted tapes, finding an effect for some conditions.

Manglik and Bergles (1992a) presented a very comprehensive discussion on the influence of twisted tapes on laminar flow and heat transfer, proposing the most general and accurate prediction methods available and those recommended for use here. They proposed the upper bound of laminar flow with twisted tape inserts to be given by

$$Sw = \frac{Re_S}{\sqrt{y}} = \left(\frac{Re}{\sqrt{y}}\right)\left(\frac{\pi}{\pi - (4\delta/d_i)}\right)\left(1 + \left(\frac{\pi}{2y}\right)^2\right)^{1/2} \cong 1400 \qquad [4.7.3]$$

In this expression, Sw is the swirl number, Re_S is the swirl Reynolds number, δ is the thickness of the twisted tape and y is the twist ratio while Re is the Reynolds number for the tube without the twisted tape present. According to them, the Swirl number represents the force ratio of

$$Sw = \left(\frac{(\text{centrifugal force})(\text{convective inertia force})}{(\text{viscous force})^2}\right)^{1/2} \qquad [4.7.4]$$

They proposed the following equation to predict the isothermal friction factors for fully developed laminar swirl flow:

$$f_S\, Re_S = 15.767\left(\frac{\pi + 2 - (2\delta/d_i)}{\pi - (4\delta/d_i)}\right)^2 \left(1 + 0.000001\, Sw^{2.55}\right)^{1/6} \qquad [4.7.5]$$

For a straight insert without twist, Sw → 0 as y → ∞, so that the last term in this expression goes to unity, for which their solution then matches that for fully developed laminar flow in a half tube (semi-circular duct). This expression predicted experimental results from three different studies with twist ratios from 3.0 to ∞ to within ±10%. Presumably, the same viscosity ratio correction can be applied to the isothermal friction factor of the twisted tape as was used for plain straight tubes above. The pressure drop in a tube of length L with a twisted tape is calculated as:

$$\Delta p = \frac{f_S d_i}{2\rho U_S^2 L_S} \qquad [4.7.6]$$

In this expression, the flow path length of a helical streamline L_S in a tube with a twisted tape insert compared to the straight length of the tube L is given by:

$$L_S = L\left[1 + \left(\frac{\pi}{2y}\right)^2\right]^{1/2} \qquad [4.7.7]$$

Similarly, the swirl velocity U_{Sw} is given by:

$$U_S = U\left[1 + \left(\frac{\pi}{2y}\right)^2\right]^{1/2} \qquad [4.7.8]$$

The actual velocity U in the tube is that given by the cross-sectional area of the tube minus that occupied by the tape:

$$U = \frac{\dot{m}}{\rho\left(\pi d_i^2/4 - \delta d_i\right)} \qquad [4.7.9]$$

The mean Nusselt number for twisted tape inserts for laminar flow heat transfer with a uniform wall temperature condition (T) is given by their expression:

$$Nu_{T,tt} = \frac{\alpha_{tt} d_i}{k} = 4.612\left\{\begin{bmatrix}\left(1 + 0.0951 Gz^{0.894}\right)^{2.5} + \\ 0.000000006413\left(Sw\,Pr^{0.391}\right)^{3.835}\end{bmatrix}^{2.0} + 0.00000000000002132\left(Re\,Ra\right)^{2.23}\right\}^{0.1}\left(\frac{\mu_{bulk}}{\mu_{wall}}\right)^{0.14} \qquad [4.7.10]$$

In this expression, Re is refers to the actual Reynolds number accounting for the blockage of the tape in the tube, that is $Re = \rho U d_i/\mu$. The Graetz number is defined as:

$$Gz = \frac{\dot{m} c_p}{k L} \qquad [4.7.11]$$

The Rayleigh number includes the buoyancy effects on heat transfer using the coefficient of thermal expansion β and the wall-to-bulk temperature difference and is defined as:

$$Ra = \left(\frac{g \rho^2 d_i^3 \beta \left|T_{wall} - T_{bulk}\right|}{\mu^2}\right) Pr \qquad [4.7.12]$$

The experimental database for this method covered three different experimental studies including ethylene glycol, water, and Polybutene 20 for twist ratios from 3.0 to ∞, predicting nearly all the data to be within ±15%.

4.8 Laminar Heat Transfer with Wire Mesh Inserts

Wire mesh inserts developed by Cal Gavin Ltd. have been successfully applied to laminar flows now for several decades in a wide range of applications and are an excellent option for enhancing heat transfer in laminar flows. These inserts tend to yield much higher heat transfer and pressure drop augmentation ratios than twisted tape inserts. However, these are not described here since the design methods are not in the public domain; the reader is referred to Cal Gavin Ltd. for a description of the inserts and thermal design information.

4.9 Laminar Heat Transfer in Internally Finned Tubes

Internally finned tubes for application to laminar flows have not been widely investigated in the literature. Marner and Bergles (1985) surveyed the literature at that time, finding only a handful of experimental studies. For example, Watkinson, Milleti and Kubanek (1975) and Soliman and Feingold (1977) carried out tests on specific fin geometries. Choudhury and Patankar (1985) and MacArthur and Patankar (1985) numerically investigated laminar flow and heat transfer inside internally finned tubes and spiral annular passages, respectively. In the first study, they noted significant buoyancy (natural convection) effects in a developing laminar flow, primarily on heat transfer but less so on pressure drop. In the second study, with

fins in the annulus of a double-pipe heat exchanger, they analyzed the effect of the twist (or spiral) of the fins on pressure drop and heat transfer relative to straight fins, finding that for some conditions the Poiseuille number (Po = f Re) in spiral fins was doubled while the heat transfer was up to five times higher, both created by the secondary flow effects. This work points to the high heat transfer augmentation effects that may potentially be created by internal fins, either inside tubes or in annuli.

In perhaps the detailed experimental study, Marner and Bergles (1985) tested one internally finned tube with a highly viscous fluid (Polybutene 20). The tests were done under constant wall temperature conditions. Their 25.1 mm internal diameter, finned tube had 16 spiral fins of 0.66 mm thickness and 2.08 mm height with a spiral fin pitch of 88.9 mm. The isothermal friction factors for this tube were 1.7 times those of a comparable diameter plain tube. For heat transfer, the finned tube provided values 3 to 4 times higher than a plain tube when heating the fluid while only a marginal improvement when cooling. During heating, they cited the increased heat transfer surface area of the fins, a beneficial viscosity ratio effect and a swirl effect as being the primary reasons for the higher performance. For cooling this viscous fluid, they instead noted that this fluid apparently tended to "freeze" in the region between the fins, negating the influence of the fins, so that the principal effect on enhancement was only the effective reduction in the tube diameter. Correlations were proposed for the friction factor and heat transfer for this tube, plus viscosity ratio effects of the wall temperature, but these correlations are specific to this one tube and cannot be generalized for use with other internally finned tubes. The interested reader is referred to the original paper for these methods.

In summary, internally finned tubes (and finned annuli) may provide a significant augmentation in heat transfer and pressure drop. However, it seems that they are best used when the fluid is being heated but not when it is being cooled. So far, apparently no general prediction method is available to handle the effects of the fin geometry (number of fins, fin height, fin thickness, fin shape, etc.).

4.10 Laminar Heat Transfer in Spirally Fluted Tubes

These spirally fluted tubes (and corrugated tubes) have not seen a significant research effort in the literature. Bergles (1981) presented a detailed survey of heat transfer characteristics of deep spirally fluted tubes. Another review is available in Garimella and Christensen (1992). Spirally fluted tubes for laminar flows were also addressed in the review by Bergles, Webb and Junkhan (1979).

With respect to experimental studies, according to the aforementioned reviews by Bergles, for laminar flows inside a Turbotec spirally fluted tube, heat transfer was increased by up to two times compared to a plain tube when heating the test fluid (Alta-Vis-530) but no improvement was found when cooling the same fluid. Rozalowski and Gater (1975) made tests on a deeply grooved flexible hose in laminar flow with two highly viscous fluids (Zerolene SAE-50 and Alta-Vis-530), finding up to three times heat transfer augmentation during heating, no augmentation when cooling Alta-Vis-530 but up to 100% higher performance when cooling the Zerolene. Even earlier than that, Kalinin and Yarkho (1971) studied deeply deformed tubes with transverse ridges for laminar flow with water, which from limited data showed that three of the seven configurations actually reduced heat transfer rather than augmented it.

With respect to pressure drop in laminar flows, several experimental studies with deep spirally fluted tubes are available. Rozalowski and Gater (1975) found pressure drops to be about four times those of the equivalent diameter plain tube. Kliebe (1978) found isothermal pressure drops from 2 to 4 times higher for the Turbotec tube with Alta-Vis-530. For a large selection of spirally fluted tubes used as the inside tube of an annulus with water as the test fluid, Garimella and Christensen (1992) found pressure drop multipliers to range from 1.1 to 2.0 and also noted that the transition to turbulent flow occurred at a much lower Reynolds number in the range from 310 to 1000.

Based on the wide variety of spirally fluted geometries and shapes, it is not possible apparently to provide a general method for predicting their heat transfer and pressure drop characteristics. Methods have been proposed in some of the above-mentioned experimental papers, but each method is limited to the particular type of flute shape and usually only one tube sample. Thus, no prediction methods are presented here for spirally fluted tubes.